

## On-Line Alpha Spectroscopy of Neutron-Deficient Actinium Isotopes\*

KALEVI VALLI, WILLIAM J. TREYTL,† AND EARL K. HYDE

Lawrence Radiation Laboratory, University of California, Berkeley, California

(Received 6 October 1967)

Isotopes of actinium lighter than mass 216 were studied at the Berkeley heavy-ion linear accelerator by bombardment of  $^{209}\text{Bi}$  with  $^{12}\text{C}$ , enriched  $^{205}\text{Tl}$  and  $^{203}\text{Tl}$  with  $^{16}\text{O}$ , and  $^{197}\text{Au}$  with  $^{20}\text{Ne}$ . Silicon (Au) surface-barrier detectors were used in on-line measurements to determine  $\alpha$ -decay characteristics. Mass-number assignments of  $^{209}\text{Ac}$  through  $^{215}\text{Ac}$  were made on the basis of excitation functions, genetic relationships with radium isotopes, and systematic trends in  $\alpha$ -decay energies. Half-lives and  $\alpha$ -particle energies were determined.

### I. INTRODUCTION

IN a series of previous investigations, we have studied  $\alpha$ -decay properties of neutron-deficient isotopes of polonium and astatine,<sup>1</sup> radon,<sup>2</sup> francium,<sup>3</sup> and radium<sup>4</sup> using on-line techniques at the Berkeley heavy-ion linear accelerator (HILAC). In this paper, we discuss the extension of the work to the light isotopes of actinium about which little is known.<sup>5</sup> The only available experimental information is an unpublished study of Griffioen and Macfarlane<sup>6</sup> in which  $\alpha$  energies and half-lives were determined for  $^{214}\text{Ac}$  and  $^{213}\text{Ac}$ , and a recent study of  $^{216}\text{Ac}$  by Rotter *et al.*<sup>7</sup>

In the present study, a number of new  $\alpha$  groups were found among the products of gold, thallium, and bismuth targets bombarded with  $^{20}\text{Ne}$ ,  $^{16}\text{O}$ , and  $^{12}\text{C}$ , respectively. These new activities were assigned to the actinium isotopes  $^{209}\text{Ac}$  through  $^{215}\text{Ac}$ , and half-lives and accurate  $\alpha$  energies were determined for them.

The new information is interesting in its own right and is valuable in connection with the method of closed  $\alpha$ - $\beta$  decay cycles for improving and extending estimates of atomic masses,  $\alpha$ - and  $\beta$ -decay energies, and neutron- and proton-binding energies.<sup>8</sup> The present data are useful as a preparation for the study of isotopes of thorium and protactinium, because light actinium isotopes occur among the decay and by-products in such studies. The information is also important in connection with experimental attempts to prepare new isotopes of elements beyond atomic

number 100 by reactions induced by complex nuclear projectiles (heavy ions), because traces of lead or bismuth in the target material can cause the formation of  $\alpha$ -active isotopes of many elements in the group between lead and thorium.

### II. EXPERIMENTAL

Our experimental technique was similar to the methods used by Ghiorso,<sup>9</sup> and Macfarlane and Griffioen.<sup>10</sup> Essentially, the reaction products recoiling from a thin target were slowed down to thermal energies in a helium atmosphere and swept through a small nozzle onto a catcher foil in an adjacent vacuum chamber. The products thus deposited were then positioned within about 0.1 sec in front of a Si(Au) surface-barrier detector. Small amounts of activity were collected on the catcher foil in less than 50 msec, while the collection time for the major part was of the order of seconds. In a typical experiment recoil activity was alternatively collected for a fraction of a second and counted for the same period, with the cycle repeated over a period of 5 to 40 min. The apparatus, electronics, and the special energy calibration method are described in a previous article.<sup>1</sup> The energy standards used to

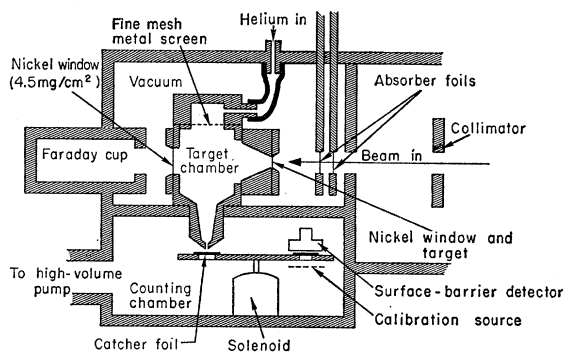


FIG. 1. Schematic diagram of improved apparatus for rapid collection of recoil activity. For  $^{197}\text{Au} + ^{20}\text{Ne}$  reactions the following values were used: chamber depth from target to back window, 3.6 cm; absolute helium pressure, 1.7 atm; helium flow rate, 90  $\text{cm}^3/\text{sec}$ . For other reactions the helium pressure was varied to obtain maximum yields.

<sup>9</sup> A. Ghiorso (unpublished).

<sup>10</sup> R. D. Macfarlane and R. D. Griffioen, Nucl. Instr. Methods 24, 461 (1963).

\* Work done under the auspices of the U. S. Atomic Energy Commission.

† Present address: U. S. Naval Radiological Defense Laboratory, San Francisco, Calif.

<sup>1</sup> W. Treytl and K. Valli, Nucl. Phys. A97, 405 (1967).

<sup>2</sup> K. Valli, M. J. Nurmi, and E. K. Hyde, Phys. Rev. 159, 1013 (1967).

<sup>3</sup> K. Valli, E. K. Hyde, and W. Treytl, J. Inorg. Nucl. Chem. 29, 2503 (1967).

<sup>4</sup> K. Valli, W. Treytl, and E. K. Hyde, Phys. Rev. 161, 1284 (1967).

<sup>5</sup> E. K. Hyde, I. Perlman, and G. T. Seaborg, *The Nuclear Properties of Heavy Elements* (Prentice-Hall, Inc., Englewood Cliffs, N. J., 1964), Vol. II, pp. 1104-1107.

<sup>6</sup> R. D. Griffioen and R. D. Macfarlane (unpublished) (cf. Ref. 5).

<sup>7</sup> Kh. Rotter, A. G. Demin, L. P. Pashchenko, and Kh. F. Brinkmann, *Yadern. Fiz.* 4, 246 (1966) [English transl.: Soviet J. Nucl. Phys. 4, 178 (1967)].

<sup>8</sup> V. E. Viola, Jr., and G. T. Seaborg, J. Inorg. Nucl. Chem. 28, 697 (1966).

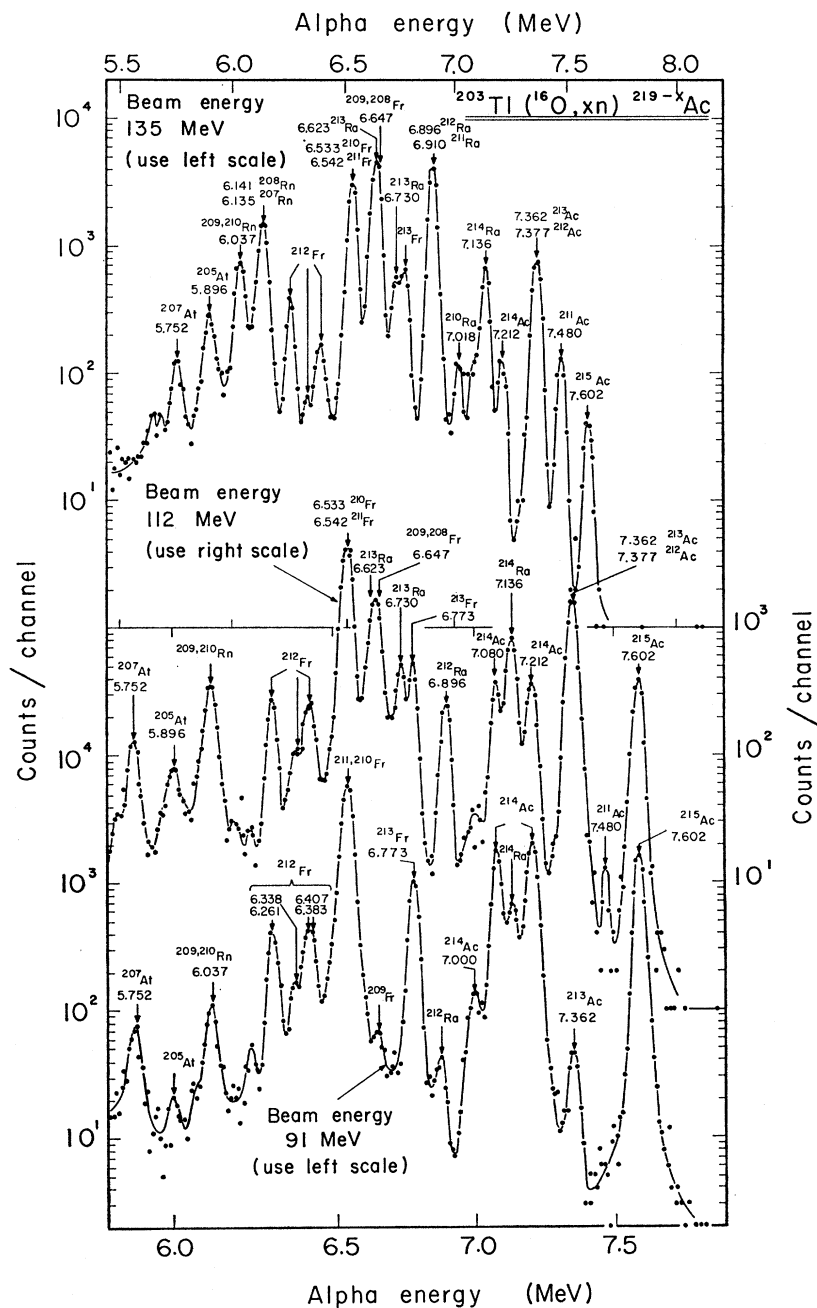


FIG. 2. Three  $\alpha$  spectra showing actinium, radium, and francium activities from the  $^{203}\text{Tl}(^{16}\text{O},xn)^{219-x}\text{Ac}$  reactions. At 91- and 112-MeV beam energies the beam current,  $0.25 \mu\text{A}$ , was integrated over the measuring time, about 17 min, to the same total in both measurements. At 135-MeV beam energy the measuring time and the total integrated beam were doubled; the  $\alpha$  energy scale was also different. Two catcher foils were flipped between alternate collection and measuring positions at the rate of twice per second. These spectra and others, all taken with the new fast apparatus, were used to construct the excitation functions shown in Fig. 5.

calibrate the  $\alpha$  spectra are given in the heading of Table I.

After many sets of experiments had been completed with this apparatus, it became clear that more satisfactory results could be obtained with a redesigned apparatus with a shorter collection time. Hence we built the apparatus sketched in Fig. 1. The two essential changes consisted in a great reduction in the volume of the helium-filled chamber and the introduction of the helium at the top of the chamber through a double thickness of electromesh grid which removed some of

the turbulence from the helium flow and served to direct it in a more linear path toward the nozzle at the bottom. The conical beam entry arm of the chamber was made in several sizes and tested in a series of experiments to determine which size would give the highest yield for the activities with less than 0.5-sec half-life. Marked improvements in counting rate up to a factor of 10 or more were obtained. From the dimensions of the chamber and the helium-flow rate we compute that it requires 0.3 sec to replace the gas in the complete chamber volume.

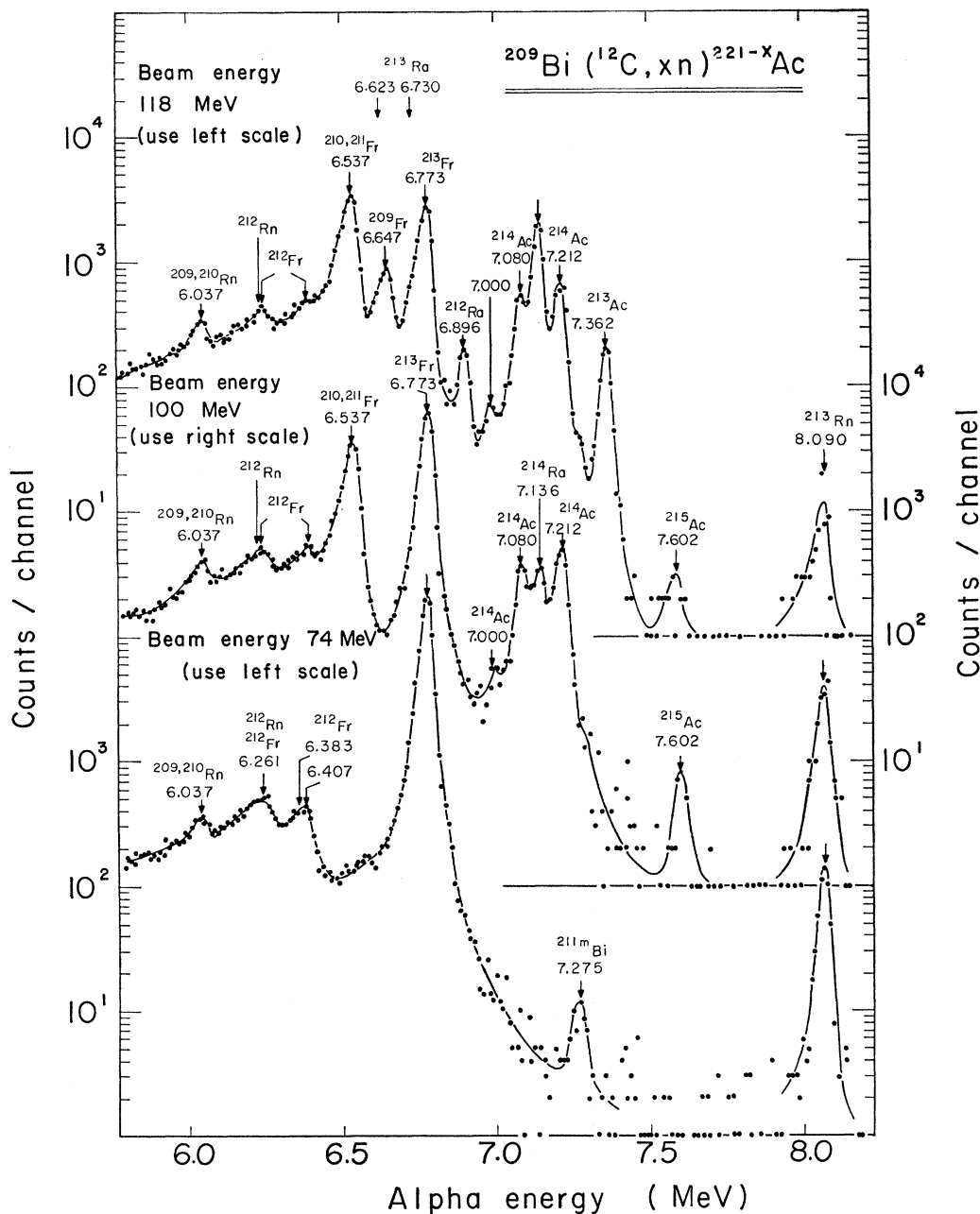
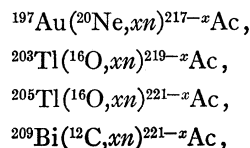


FIG. 3.  $\alpha$  spectra showing actinium, radium, and francium activities from the  $^{209}\text{Bi}(^{12}\text{C}, xn)^{221-x}\text{Ac}$  reactions at three beam energies. The beam current was integrated over the measuring time, 6 min, to the same total in each measurement. Two catcher foils were flipped between alternate collection and measuring positions at a rate of once per second. These spectra and others were used to construct the excitation functions shown in Fig. 8. The original apparatus was used.

We indicate in the figure captions and the text which data were taken with the old and which with the new apparatus.

The reactions used in the study were



where  $x$  refers to the number of evaporated neutrons. The gold target was 2.5 mg/cm<sup>2</sup> leaf. The thallium targets were separated  $^{203}\text{Tl}$  and  $^{205}\text{Tl}$  (88.2%  $^{203}\text{Tl}$ , 11.8%  $^{205}\text{Tl}$  and 99.0%  $^{205}\text{Tl}$ , 1.0%  $^{203}\text{Tl}$ , respectively, according to the supplier, Oak Ridge National Laboratory) evaporated on 2.3 mg/cm<sup>2</sup> nickel foil. The thickness of the  $^{203}\text{Tl}$  target was about 0.8 mg/cm<sup>2</sup> and that of  $^{205}\text{Tl}$  about 1.0 mg/cm<sup>2</sup>. The bismuth target was 2.26 mg/cm<sup>2</sup> natural bismuth evaporated on 1.92 mg/cm<sup>2</sup> aluminum foil.

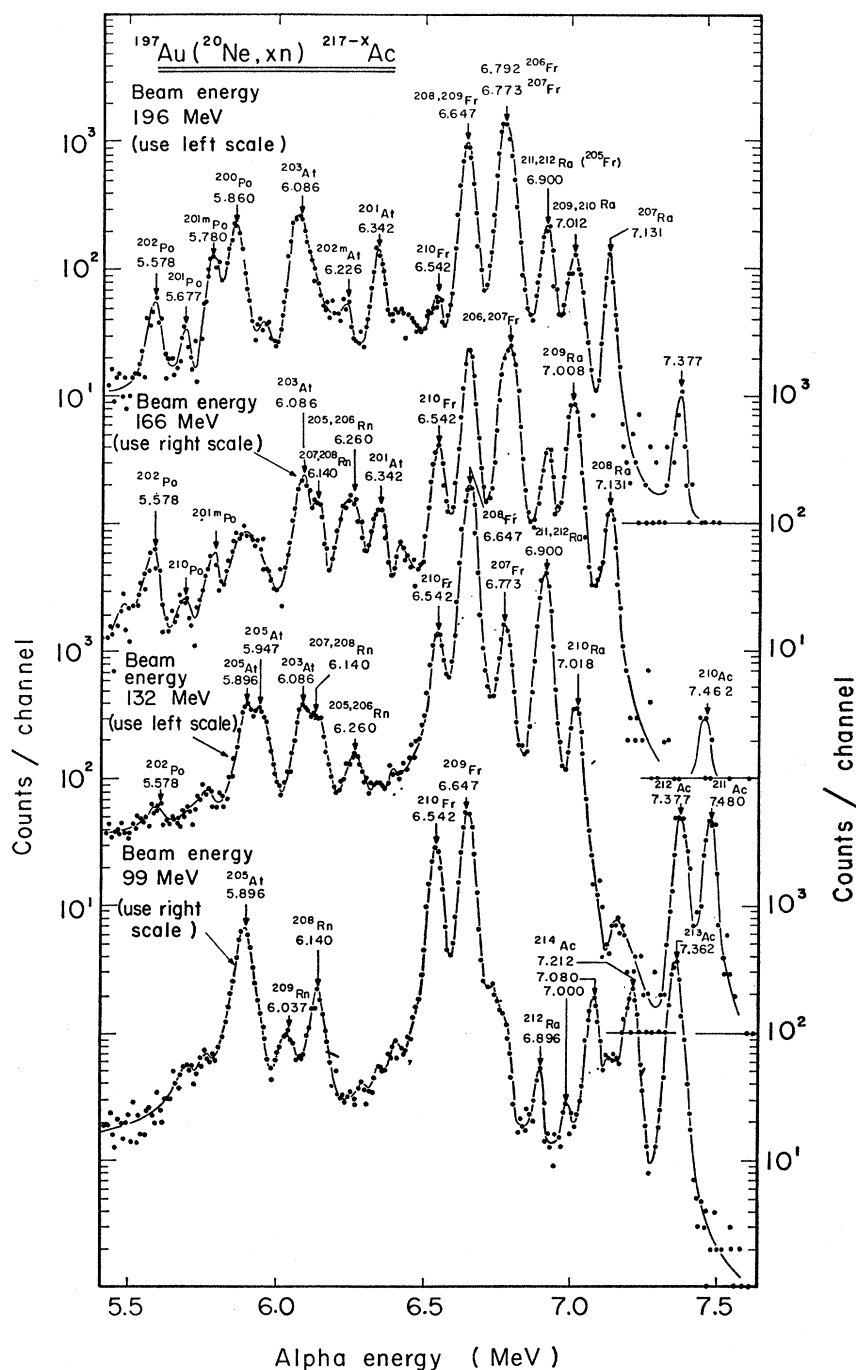


FIG. 4.  $\alpha$  spectra showing actinium, radium, and francium activities from the  $^{197}\text{Au}(^{20}\text{Ne}, xn)^{217-x}\text{Ac}$  reactions at three beam energies. The beam current,  $0.8 \mu\text{A}$ , was integrated over the measuring time, about 36 min, to the same total in each measurement. Two catcher foils were flipped between alternate collection and measuring positions at the rate of twice per second. The original apparatus was used.

The maximum beam energy was 208 MeV for  $^{20}\text{Ne}$ , 166 MeV for  $^{16}\text{O}$ , and 125 MeV for  $^{12}\text{C}$ . Lower energies were obtained by inserting stacks of  $1.72 \text{ mg/cm}^2$  aluminum absorber foils in front of the target.<sup>1</sup> The range-energy relationships of Northcliffe<sup>11,12</sup> were used to calculate the energy degradation in the absorbers.

The yield versus beam energy curves were measured

starting at the Coulomb barrier and progressively increasing the beam energy until the maximum energy was reached, or vice versa, starting at full beam energy and ending at the barrier. The total integrated beam current was the same for all runs. The measuring time was typically 10 to 30 min and the interval between measurements 3 to 5 min.

In separate experiments half-lives of individual  $\alpha$  peaks were determined with the techniques outlined in a previous article.<sup>1</sup>

<sup>11</sup> L. C. Northcliffe, Phys. Rev. **120**, 1744 (1960).

<sup>12</sup> L. C. Northcliffe, Ann. Rev. Nucl. Sci. **13**, 67 (1963).

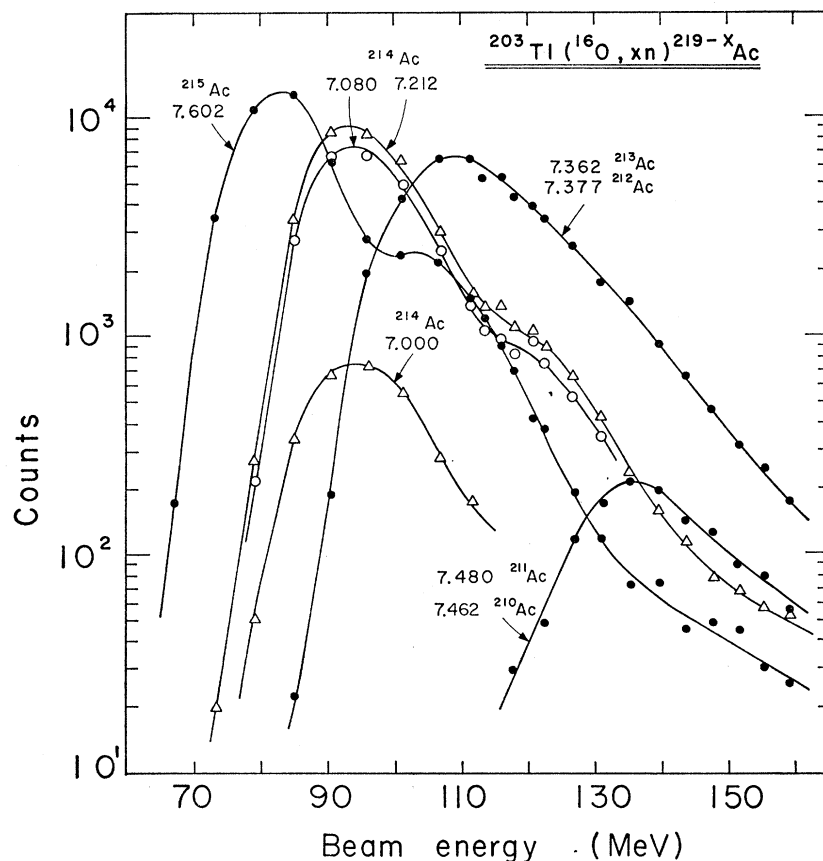


FIG. 5. Excitation functions for the actinium isotopes produced in the  $^{203}\text{Tl}(^{16}\text{O}, xn)^{219-x}\text{Ac}$  reactions. The measurements were run with the new fast apparatus from low to high-beam energies in two different sets of experiments: One extended from the Coulomb barrier to 121 MeV, the other from 113 to 159 MeV. Each point corresponds to the same total integrated beam current,  $0.25 \mu\text{A}$  during about 17 min, and the interval between successive measurements was 4 to 7 min. The second maxima came from the 11.8%  $^{206}\text{Tl}$  present in the target. The nominal Coulomb barrier from a simple tangent spheres estimate is 74 MeV. See the caption of Fig. 2 for more details.

### III. RESULTS

#### A. Experimental Data

The actinium isotopes studied in this work were far from  $\beta$  stability and had large decay energies for electron capture and  $\alpha$  decay. Accordingly, the half-lives were short: of the same order of magnitude as the collection time of our apparatus, or shorter. Particularly in the experiments performed with our original chamber, most of the actinium recoil nuclei decayed in flight before being detected, which made the daughter activities and other products of the nuclear reactions much more prominent than actinium in the spectra. Noncompound-nucleus reactions appeared to contribute more to the yields of the daughter activities than in our previous studies of elements below actinium. Hence our measurements on the actinium  $\alpha$  peaks were useful for  $\alpha$ -energy and half-life determinations and for assignment of the activities to isotopes, but not for the estimation of cross sections or branching ratios for  $\alpha$  decay and electron capture.

Figure 2 shows  $\alpha$  spectra obtained from the  $^{203}\text{Tl}+^{16}\text{O}$  reactions at three beam energies. Figure 3 shows three spectra from the  $^{209}\text{Bi}+^{12}\text{C}$  reactions, and Fig. 4 shows four spectra from the  $^{197}\text{Au}+^{20}\text{Ne}$  reactions. Besides these spectra, additional ones were taken at many

other beam energies, and the data were used in the formulation of the excitation functions. The excitation functions of the actinium isotopes from the  $^{203}\text{Tl}+^{16}\text{O}$  reactions are given in Fig. 5; the yield curves of their radium and francium daughters are shown in Fig. 6. Excitation functions for the products of the  $^{205}\text{Tl}+^{16}\text{O}$  and  $^{209}\text{Bi}+^{12}\text{C}$  reactions are given in Figs. 7 and 8, respectively. The  $^{197}\text{Au}+^{20}\text{Ne}$  reactions required two figures: The yield curves of actinium, radium, and radon are shown in Fig. 9; those of actinium, francium, and astatine are presented in Fig. 10. The curves in Figs. 2, 5, 6, 9, and 10 were obtained with the fast apparatus, those in Figs. 3, 4, 7, and 8 with the original apparatus.

#### B. General Comments on the Data

In general, the excitation functions of the activities that we have assigned to actinium isotopes have the shape typical for compound-nucleus reactions. In a given reaction each  $\alpha$  activity has a beam energy at which its yield is a maximum, and as the beam energy is raised above this, another product rises in yield. We cannot rule out some distortion of our experimental curves resulting from unknown factors in the collection of such short-lived activities. Since the mass number of the

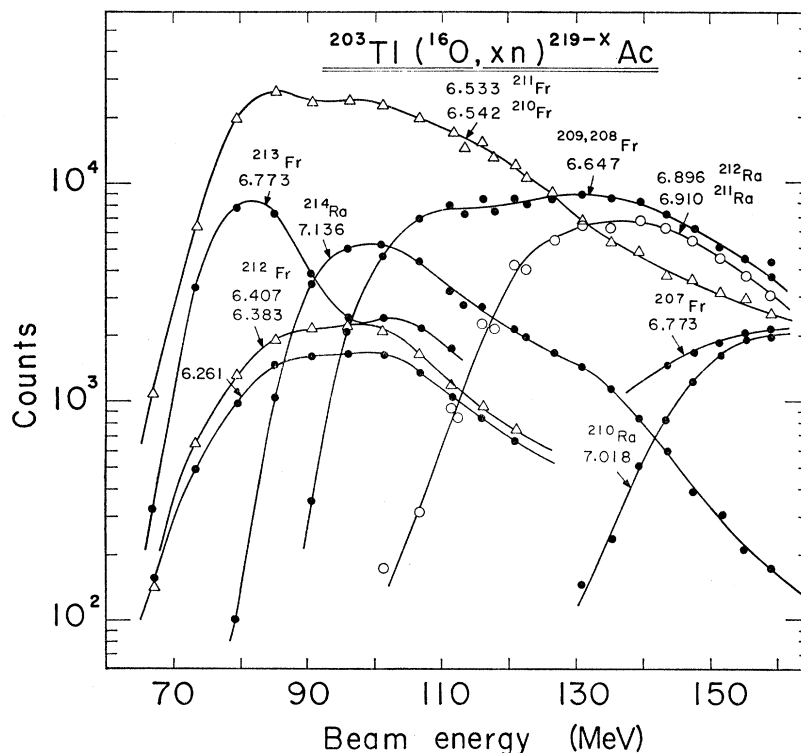


FIG. 6. Excitation functions of radium and francium activities produced in the  $^{203}\text{Tl}(^{16}\text{O}, xn)^{219-x}\text{Ac}$  reactions. See the captions of Figs. 2 and 5 for details.

compound nucleus varies from 217 to 221 in the four target-projectile systems, the maximum yield for a given product naturally occurs at different beam energies, but the order of excitation of the products stays the same. These considerations make it possible to make a preliminary association of mass numbers to the new activities or at the very least to arrange them in descending order of mass number.

The next step is to compare the curves for the actinium isotopes with the curves for the electron-capture (EC) daughter products (radium activities) and the  $\alpha$ -decay daughter products (francium isotopes). Conclusions from the comparison of these curves must

be made with some caution owing to a difficulty which is explained with the aid of Fig. 11. In this figure, the  $\alpha$ -disintegration energy is plotted versus neutron number for several elements in the mass-number range in which our products lie. The topmost curve includes our new data on actinium isotopes with the assignments as given below. A striking feature of this figure is the step effect. Neighboring isotopes have closely similar  $\alpha$  energies (and often closely similar half-lives), so that it is difficult to distinguish the two within the  $\alpha$  energy and time resolution of our methods. Hence several of the experimental spectra and excitation functions of the francium and radium daughter peaks are composite,

TABLE I. Present results compared with previous reports. Following  $\alpha$ -energy standards were used:  $^{212}\text{Po}$  8.7854 MeV,  $^{215}\text{Po}$  7.3841 MeV,  $^{219}\text{Rn}$  6.8176 MeV,  $^{211}\text{Bi}$  6.6222 MeV.<sup>a</sup>

Isotope	$\alpha$ energy (MeV)	This work		Griffioen and Macfarlane <sup>b</sup>		
		Half-life (sec)	%	$\alpha$ energy (MeV)	Half-life (sec)	%
$^{216}\text{Ac}$	$7.602 \pm 0.005$	$0.17 \pm 0.01$		$9.14 \pm 0.03^c$	$0.39 \pm 0.03$ msec <sup>c</sup>	
$^{215}\text{Ac}$	$7.212 \pm 0.005$	$8.2 \pm 0.2$	$52 \pm 2$	7.24	12	33
$^{214}\text{Ac}$	$7.080 \pm 0.005$	$8.2 \pm 0.2$	$44 \pm 2$	7.18	12	33
	$7.000 \pm 0.015^d$	$8.2 \pm 0.5$	$4 \pm 1$	7.12	12	33
$^{213}\text{Ac}$	$7.362 \pm 0.008$	$0.80 \pm 0.05$		7.42	$\sim 1$	
$^{212}\text{Ac}$	$7.377 \pm 0.008$	$0.93 \pm 0.05$				
$^{211}\text{Ac}$	$7.480 \pm 0.008$	$0.25 \pm 0.05$				
$^{210}\text{Ac}$	$7.462 \pm 0.008$	$0.35 \pm 0.05$				
$^{209}\text{Ac}$	$7.585 \pm 0.015$	$0.10 \pm 0.05$				
$^{215}\text{Ra}$	$8.70 \pm 0.02$			8.7	1.6 msec	

<sup>a</sup> A. Rytz, *Helv. Phys. Acta* **34**, 240 (1961).

<sup>b</sup> Reference 6.

<sup>c</sup> Values for  $^{216}\text{Ac}$  come from the work of Rotter *et al.* (Ref. 7).

<sup>d</sup> This peak is probably complex.

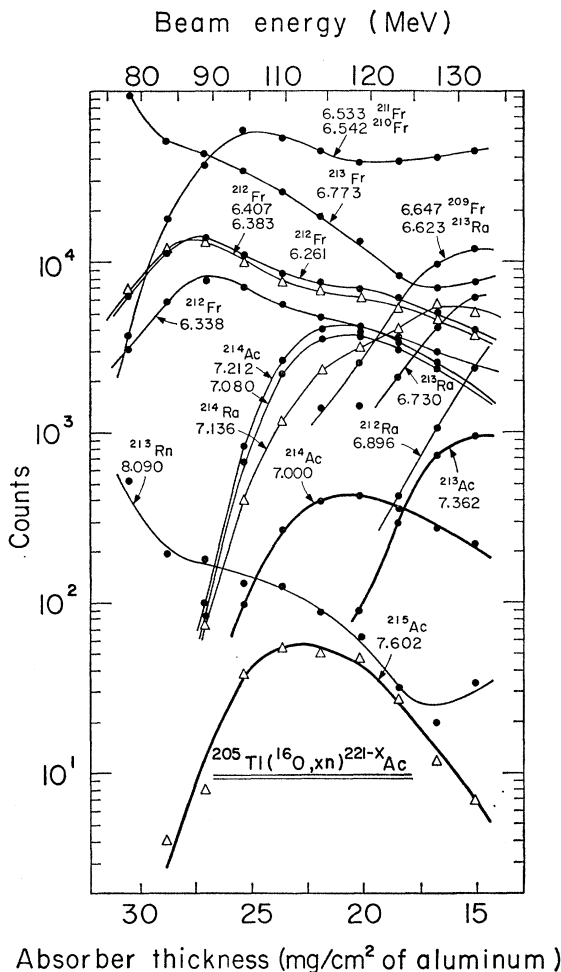


FIG. 7. Excitation functions of actinium, radium, and francium activities produced in the  $^{205}\text{Tl}(^{16}\text{O}, xn)^{221-x}\text{Ac}$  reactions. The experiments were run from low- to high-beam energies with 3- to 4-min intervals between measurements. The beam current,  $0.4\ \mu\text{A}$ , was integrated over the measuring time, about 15 min, to the same total in each measurement. Two catcher foils were flipped between alternate collection and measuring positions at the rate of twice per second. The original apparatus was used.

and it is not obvious which mass number to associate with the daughter and hence which mass number to attribute to the actinium parent. To complicate matters, the form of several of the yield curves for the francium isotopes is such as to suggest some direct production via reactions of the (heavy ion,  $\alpha xn$ ) and (heavy ion,  $p xn$ ) types. Our comments on these matters are collected in Sec. IV.

However, we believe that we can make definite mass assignments to the new actinium activities on the basis of the arguments outlined in the section which follows. A summary of our assignments is given in Table I, where they are compared with the unpublished results of Griffioen and Macfarlane.<sup>6</sup> The quoted errors are conservative limits covering the total spread of several individual measurements and are substantially greater than the statistical uncertainty.

### C. Evidence for Specific Mass Assignment

#### Actinium-215

From the observed regularities in the  $\alpha$ -decay properties of the known polonium, astatine, radon, francium, and radium isotopes (see Fig. 11) one expects the isotope  $^{215}\text{Ac}$ , containing 126 neutrons, to emit an

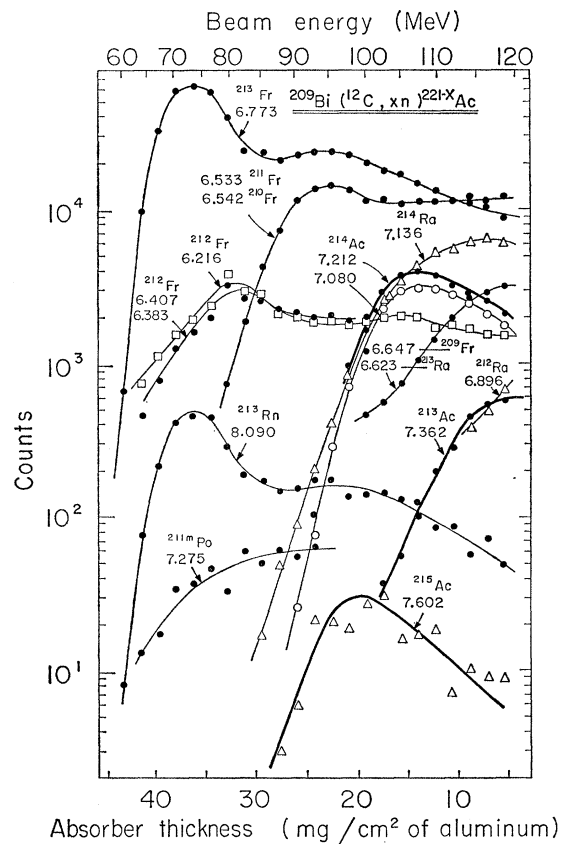


FIG. 8. Excitation functions of actinium, radium, and francium activities produced in the  $^{209}\text{Bi}(^{12}\text{C}, xn)^{221-x}\text{Ac}$  reactions. The experiments were run with the original apparatus from high- to low-beam energies with 3-min intervals between the measurements. See the caption of Fig. 3 for more details. The nominal Coulomb barrier from a simple tangent spheres estimate is 58 MeV.

$\alpha$  particle of about 7.60 MeV. An  $\alpha$ -particle group with 7.602-MeV energy and  $0.17 \pm 0.01$ -sec half-life was observed in the  $^{203}\text{Tl}+^{16}\text{O}$ ,  $^{205}\text{Tl}+^{16}\text{O}$ , and  $^{209}\text{Bi}+^{12}\text{C}$  reactions (see Figs. 2, 3, 5, 7, and 8).

The shape of the excitation function for the 7.602-MeV  $\alpha$  activity in the  $^{203}\text{Tl}+^{16}\text{O}$  case (Fig. 5) is particularly good evidence for the assignment to  $^{215}\text{Ac}$ . The maximum yield occurs at 83-MeV bombarding energy, 9 MeV above the Coulomb barrier, and rapidly decreases at higher energies; the second maximum is caused by the 11.8%  $^{205}\text{Tl}$  in the target. At a bombarding energy of 83 MeV, the excitation energy of the  $^{219}\text{Ac}$  compound nucleus is 43 MeV, which is reasonable for the evaporation of four neutrons. Evaporation of only

three neutrons would result in the formation of  $^{216}\text{Ac}$  which is known from the work of Rotter *et al.*<sup>7</sup> to have an  $\alpha$  energy of 9.14 MeV and a half-life of 0.39 msec.

If the 215-mass assignment is correct, the 7.602-MeV  $\alpha$  group should not appear in any spectrum from the  $^{197}\text{Au}+^{20}\text{Ne}$  reactions because the  $^{217}\text{Ac}$  compound nucleus has far too much excitation energy even at the barrier to emit only two neutrons; in keeping with this, the 7.602-MeV group was not seen in these spectra. The new activity has its maximum yield in the  $^{205}\text{Tl}+^{16}\text{O}$  reaction (Fig. 7) for a beam energy of 111 MeV and in the  $^{209}\text{Bi}+^{12}\text{C}$  case (Fig. 8) for a beam energy of 99 MeV, corresponding to excitation energies for the  $^{221}\text{Ac}$  compound nucleus of 67 and 66 MeV, respectively, which is reasonable for the evaporation of six neutrons.

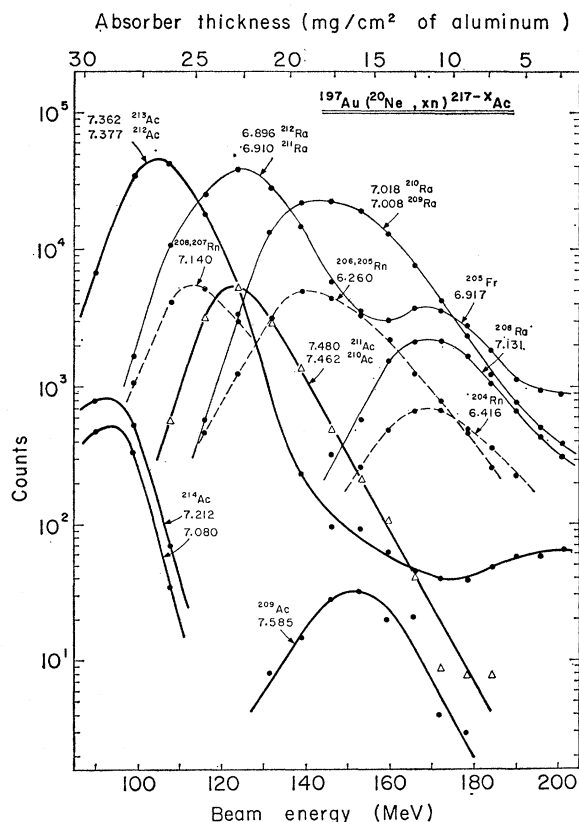


FIG. 9. Excitation functions of actinium, radium, and radon activities produced in the  $^{197}\text{Au}(^{20}\text{Ne}, xn)^{217-x}\text{Ac}$  reactions. The experiments were run from high- to low-beam energies with 5- to 7-min intervals between measurements. The beam current,  $0.8 \mu\text{A}$ , was integrated over the measuring time, about 35 min, to the same total in each measurement. Two catcher foils were flipped between alternate collection and measuring positions at the rate of twice per second. The new fast apparatus was used. The Coulomb barrier from a simple tangent spheres estimate is 88 MeV.

The  $\alpha$ -decay daughter of  $^{215}\text{Ac}$  is  $^{211}\text{Fr}$ , which emits  $\alpha$  particles of 6.533-MeV energy and 3.06-min half-life. An  $\alpha$  activity with these properties is prominent in the spectra, but the observed activity is a composite of

$^{211}\text{Fr}$  and  $^{210}\text{Fr}$  activity, the latter having an  $\alpha$ -particle energy of 6.542 MeV and 3.18-min half-life.<sup>3</sup>

The electron-capture branching of  $^{215}\text{Ac}$  to produce 1.6-msec  $^{215}\text{Ra}$  ( $E_\alpha=8.7$  MeV)<sup>6</sup> is expected to be small. In a long run with the fast apparatus using the  $^{203}\text{Tl}+^{16}\text{O}$  reaction at a 80-MeV ion energy, we observed a weak  $\alpha$  peak at  $8.70 \pm 0.02$  MeV. If we attribute this  $\alpha$  group to  $^{215}\text{Ra}$ , we obtain an electron-capture branch of  $0.09 \pm 0.02\%$  for  $^{215}\text{Ac}$ .

#### Actinium-214

In an unpublished study of the products of bismuth bombarded with carbon ions, Griffioen and Macfarlane<sup>6</sup> found evidence for  $\alpha$  groups of  $^{214}\text{Ac}$  with energies of 7.12, 7.18, and 7.24 MeV and a half-life of 12 sec. These probably correspond to the peaks at 7.080, 7.136, and 7.212 MeV visible in our spectra in Figs. 2-4. In addition, we see a small peak at 7.000 MeV. From the shape of this peak we suspect that it is composed of two groups differing in energy by 10 to 20 keV.

The excitation functions of these four peaks are shown in Figs. 5 and 7-10. The similarity of the curves for the peaks at 7.212, 7.080, and 7.000 MeV makes us conclude that they are associated with a single isotope. The maximum yield occurs at bombarding energies which

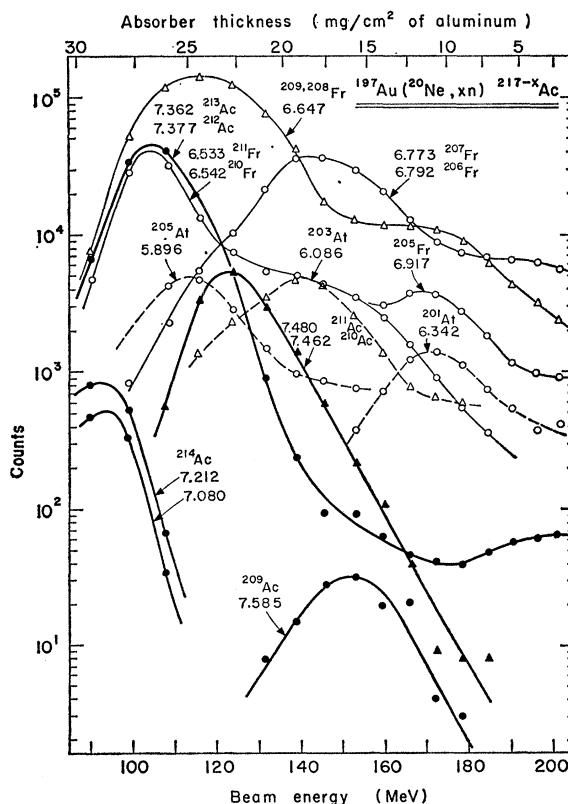


FIG. 10. Excitation functions of actinium, francium, and astatine activities produced in the  $^{197}\text{Au}(^{20}\text{Ne}, xn)^{217-x}\text{Ac}$  reactions. See the caption of Fig. 9 for details.



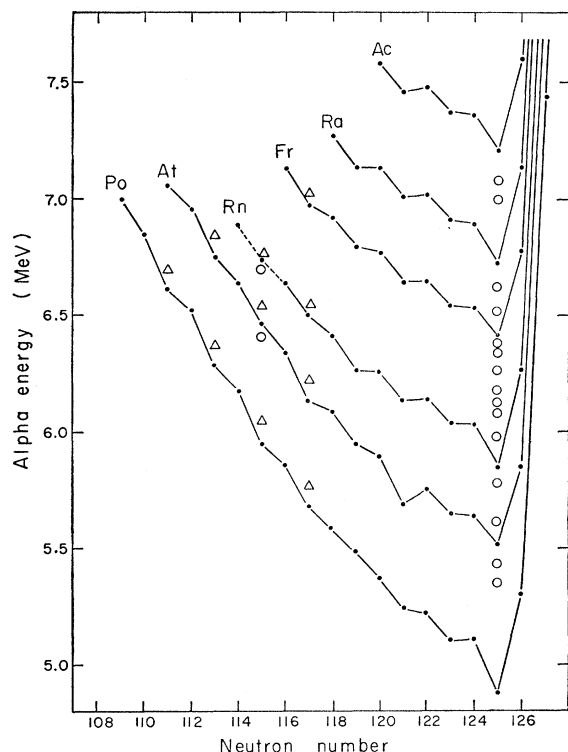


FIG. 11.  $\alpha$  energy versus neutron number for isotopes of different elements below 126-neutron shell and above 82-proton shell. The solid circles indicate energies assigned to ground-state  $\alpha$  decay. The crosses represent  $\alpha$  energies assigned to isomeric states. The open circles are  $\alpha$  transitions to excited levels at the daughter nuclei ( $\alpha$  fine structure).

are reasonable for the  $^{214}\text{Ac}$  assignment in the four reactions studied. For example, in Fig. 5, the peak yield occurs for 94-MeV  $^{16}\text{O}$  corresponding to 52-MeV excitation of the  $^{219}\text{Ac}$  compound nucleus, a reasonable excitation for the evaporation of five neutrons.

The peak at 7.136 MeV can be assigned to  $^{214}\text{Ra}$ , which is known from our previous work<sup>4</sup> to have an  $\alpha$ -particle energy of  $7.136 \pm 0.005$  MeV and a half-life of 2.6 sec. This activity appears in our spectra partly because of its formation by the electron capture of  $^{214}\text{Ac}$  and partly by some direct process. At the peak of the excitation function for  $^{214}\text{Ac}$  in the  $^{208}\text{Tl} + ^{16}\text{O}$  case (see Figs. 5 and 6) we have strong evidence that  $^{214}\text{Ra}$  is indeed formed by electron capture in the fact that the apparent half-life of the 7.136-MeV peak observed at a 90-MeV  $^{16}\text{O}$  beam energy is 8 sec; the same value obtained for the  $^{214}\text{Ac}$  peaks at 7.212, 7.080, and 7.000 MeV. Hence at this beam energy  $^{214}\text{Ra}$  is in equilibrium with its parent. On the other hand, when we raise the beam energy to 115 MeV, the  $^{214}\text{Ra}$  peak has a composite decay curve with 2.5- and 8-sec components.

The  $\alpha$ -decay daughter of  $^{214}\text{Ac}$  is  $^{210}\text{Fr}$ , which emits 6.542-MeV  $\alpha$  particles. In fact,  $\alpha$  particles of this energy are prominent in our spectra, but the energy resolution of our detector was not sufficiently good to separate the contributions of  $^{210}\text{Fr}$  and  $^{211}\text{Fr}$ . Hence we cannot make

a clear-cut statement of the relationship of the  $^{214}\text{Ac}$  and  $^{210}\text{Fr}$  activity.

The relative intensities of the  $^{214}\text{Ac}$  peaks are as follows: 7.212 MeV  $52 \pm 2\%$ , 7.080 MeV  $44 \pm 2\%$ , and 7.000 MeV  $4 \pm 1\%$ . This complex structure can be taken as additional evidence that our mass assignment is correct, if we note the fact that  $^{214}\text{Ac}$ ,  $^{213}\text{Ra}$ ,  $^{212}\text{Fr}$ ,  $^{211}\text{Em}$ , and  $^{210}\text{At}$ , all nuclides with 125 neutrons, have a roughly similar pattern of complex structure, whereas all the lighter nuclei of these elements have only one prominent  $\alpha$  group.

An estimate of the EC/ $\alpha$  ratio of  $^{214}\text{Ac}$  can be made from the ratio of  $^{214}\text{Ac}$  and  $^{214}\text{Ra}$   $\alpha$  activity in the  $^{208}\text{Tl} + ^{16}\text{O}$  reaction at beam energies of 90 MeV or less. The value obtained corresponds to an upper limit of  $11 \pm 3\%$  for electron-capture branching of  $^{214}\text{Ac}$  and to a lower limit of  $89 \pm 3\%$  for the  $\alpha$  branch. These limits are probably not far from the true values.

#### *Actinium-213 and Actinium-212*

Extrapolation of the trends in  $\alpha$ -decay energies observed for several nearby elements (see Fig. 11) to the isotopes of actinium leads to a prediction of nearly similar  $\alpha$  energies for  $^{213}\text{Ac}$  and  $^{212}\text{Ac}$  at about 7.36 MeV.

There is a peak in the  $\alpha$  spectra in Figs. 2-4 which we attribute to  $^{213}\text{Ac}$  with an energy of 7.362 MeV, to  $^{212}\text{Ac}$  with an energy of 7.377 MeV, or to a mixture of both, depending on the reaction system and the beam energy. The excitation function of the composite peak appears in Figs. 5 and 7-10. There are several reasons for believing that the excitation functions in Figs. 5, 9, and 10 comprise a mixture of  $^{213}\text{Ac}$  and  $^{212}\text{Ac}$ .

One argument for the presence of  $^{213}\text{Ac}$  in the 7.36-MeV peak is the fact that the activity begins to be produced as the energy of the beam is increased beyond that favored for the production of  $^{214}\text{Ac}$ . If  $^{213}\text{Ac}$  were the sole contributor to the observed peak, the  $\alpha$  energy and half-life should remain the same under all conditions. But there is a clear shift in the energy of the observed  $\alpha$  peak as the beam energy is changed. In a series of runs in which the energy scale was carefully and repeatedly calibrated the energy of this actinium peak was determined to be 7.362 MeV when it was prepared with 99-MeV  $^{20}\text{Ne}$  ions on gold targets and 7.377 MeV when it was prepared with 132-MeV  $^{20}\text{Ne}$  ions. We assign these energies to  $^{213}\text{Ac}$  and  $^{212}\text{Ac}$ , respectively.

The half-life of  $^{213}\text{Ac}$  was determined by measurements of the decay of its  $\alpha$  peak in samples prepared by the  $^{208}\text{Tl} + ^{16}\text{O}$  reaction at a beam energy of 105 MeV, while that for  $^{212}\text{Ac}$  was determined for samples prepared at a beam energy of 134 MeV; values of  $0.80 \pm 0.05$  sec and  $0.93 \pm 0.05$  sec, respectively, were obtained.

Furthermore the broad maximum in the  $^{209,208}\text{Fr}$  peak centered at 118 MeV in the  $^{197}\text{Au} + ^{20}\text{Ne}$  reactions (Fig. 10) is most probably a reflection of the formation of these isotopes from  $\alpha$  decay of  $^{213}\text{Ac}$  and  $^{212}\text{Ac}$ . An

argument can also be made from the behavior of the composite  $^{212,211}\text{Ra}$  peak in Fig. 9. In samples made at a  $^{20}\text{Ne}$  beam energy of 124 MeV an energy value of 6.896 MeV, equal to our published value for  $^{212}\text{Ra}$ , was obtained. However, we cannot rule out the possibility of substantial formation of  $^{212}\text{Ra}$  via the  $(^{20}\text{Ne}, p4n)$  reaction.

#### *Actinium-211 and Actinium-210*

The unknown  $\alpha$  peak which appears in our spectra at about 7.48 MeV can be assigned to  $^{211}\text{Ac}$  and  $^{210}\text{Ac}$ . The systematic trends displayed in Fig. 11 show that it is reasonable to expect these isotopes to have nearly the same  $\alpha$ -particle energy, and the following pieces of evidence help to confirm this choice.

First, we can be sure that this activity has a mass number less than 212 because it is formed at higher excitation energy in the  $^{208}\text{Tl}+^{16}\text{O}$  and  $^{197}\text{Au}+^{20}\text{Ne}$  systems than required to produce the  $^{213,212}\text{Ac}$  double peak (Figs. 5, 9, and 10). In keeping with this, the 7.48-MeV peak did not appear in any of our spectra for the  $^{205}\text{Tl}+^{16}\text{O}$  or  $^{209}\text{Bi}+^{12}\text{C}$  systems because in these cases there was not enough excitation energy, even at full beam energy, to make  $^{211}\text{Ac}$  in appreciable yield. Next, we noted a definite shift in the energy of the peak and in its half-life as the beam energy was changed. In the  $^{197}\text{Au}+^{20}\text{Ne}$  system, when we prepared the activity with 124-MeV  $^{20}\text{Ne}$  ions, the  $\alpha$  energy was 7.480 MeV. This energy we assign to  $^{211}\text{Ac}$ . When we used 145-MeV  $^{20}\text{Ne}$  ions, the  $\alpha$  energy of the unknown peak was 7.462 MeV, which we assign to  $^{210}\text{Ac}$ . We made duplicate measurements of the half-life for the 7.480-MeV activity produced at a beam energy of 124 MeV and obtained the value of  $0.25 \pm 0.05$  sec. At beam energies of 145 to 153 MeV we obtained the average value  $0.35 \pm 0.05$  sec.

The behavior of the radium isotopes provides additional support. We believe that the major fraction of the mixed  $^{212,211}\text{Ra}$  peak and the  $^{210,209}\text{Ra}$  peaks in Fig. 9 are representative of production from the electron-capture decay of actinium parent activities, although we cannot rule out independent production from  $(^{20}\text{Ne}, pxn)$  reactions. With careful energy calibration we can distinguish which radium isotope is predominant in each of these mixtures prepared at a given bombardment energy. At a  $^{20}\text{Ne}$  energy of 132 MeV,  $^{211}\text{Ra}$  is predominant in the  $^{212,211}\text{Ra}$  mixture, which is consistent with the idea that  $^{211}\text{Ac}$  is close to its peak production at that energy. The energy of the observed peak for the  $^{210,209}\text{Ra}$  mixture undergoes a steady shift from 7.018 MeV (correct for  $^{210}\text{Ra}$ ) to 7.008 MeV (correct for  $^{209}\text{Ra}$ ) as the  $^{20}\text{Ne}$  beam energy is varied from 130 to 165 MeV.

#### *Actinium-209*

In the  $^{197}\text{Au}+^{20}\text{Ne}$  series of experiments, we observed an  $\alpha$  activity with 7.585-MeV energy and a  $0.10 \pm 0.05$ -sec half-life, which we assign to  $^{209}\text{Ac}$ . A spectrum show-

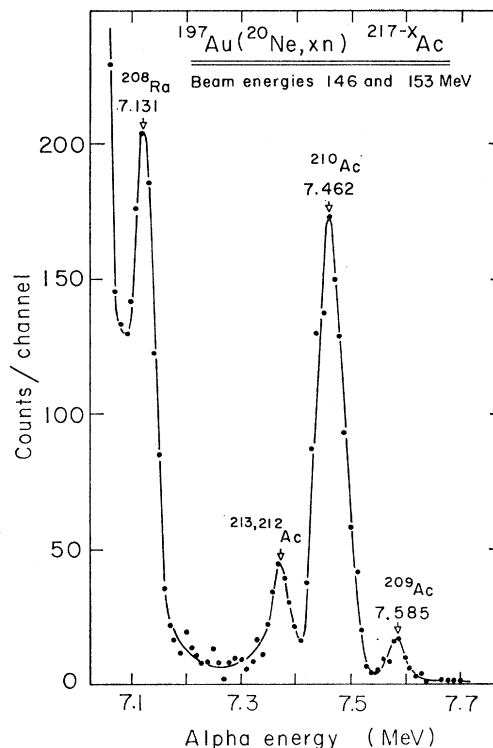


FIG. 12.  $\alpha$  spectrum showing the 7.585-MeV group of  $^{209}\text{Ac}$  from the  $^{197}\text{Au}(^{20}\text{Ne}, 8n)^{209}\text{Ac}$  reaction. The spectrum was obtained by adding together two spectra recorded at 146- and 153-MeV beam energies, respectively. The spectra were two of those used in the construction of the excitation functions shown in Figs. 9 and 10.

ing this  $\alpha$  peak is presented in Fig. 12, and the excitation function is shown in Figs. 9 and 10. The maximum yield occurs at a higher beam energy than that required for production of the composite  $^{211-210}\text{Ac}$  peak. This is reasonable but not conclusive proof for the assignment of the 7.585-MeV peak to  $^{209}\text{Ac}$ . In addition, the behavior of the composite  $^{209,210}\text{Ra}$  curve is consistent with this mass assignment. Finally, an energy of 7.585 MeV for  $^{209}\text{Ac}$  fits well with the expected systematic mass-energy behavior as exhibited in Fig. 11.

#### IV. DISCUSSION OF FRANCIUM AND RADIUM EXCITATION FUNCTIONS

Francium isotopes can be produced in these reactions in at least two ways. While the major mechanism is the  $\alpha$  decay of actinium parent nuclei, there is considerable evidence for formation by another mechanism. We call attention to particular features of our data which require this conclusion. For example, in the  $^{208}\text{Tl}+^{16}\text{O}$  reaction (see Fig. 6),  $^{213}\text{Fr}$  is produced in high yield at a bombarding energy of 80 MeV just above the barrier. This  $^{213}\text{Fr}$  cannot be formed by  $\alpha$  decay of  $^{217}\text{At}$  because the compound nucleus  $^{219}\text{Ac}$  has about 38 MeV of excitation energy—far too much for the emission of only two neutrons. It is not clear whether prompt  $\alpha$  emission from the compound nucleus resulting in the

production of  $^{213}\text{Fr}$  is a competitive form of de-excitation of the compound nucleus or whether the  $\alpha$  particle is released in a direct surface reaction. In the case of  $^{212}\text{Fr}$  it is possible that the shoulder of the curve at 75- to 80-MeV bombarding energy represents production from the  $\alpha$  decay of  $^{216}\text{Ac}$ , but the main yield at 95- to 100-MeV  $^{16}\text{O}$  energy cannot come from this reaction.

Switching our attention now to the  $^{211-210}\text{Fr}$  peak in Fig. 6, we note that the main yield occurs close to the barrier energy. This is quite in keeping with the fact that  $^{215}\text{Ac}$  is made in high yield at this bombarding energy and produces  $^{211}\text{Fr}$  by  $\alpha$  decay. We also believe that in the beam energy range 90 to 110 MeV where  $^{214}\text{Ac}$  has its maximum yield that  $^{210}\text{Fr}$  is made in  $\alpha$  decay of  $^{214}\text{Ac}$ . However, the  $^{211-210}\text{Fr}$  yield drops off only slowly at beam energies above this range, probably because of direct production.

Another example of contributions to francium yield from two mechanisms occurs in the  $^{212}\text{Fr}$  yield curve in the  $^{205}\text{Tl}+^{16}\text{O}$  reaction (Fig. 7). This curve appears to have a principal maximum at a bombarding energy of 88 MeV as well as a second maximum at 118 MeV. The first is at the right energy to indicate formation by  $\alpha$  decay from  $^{216}\text{Ac}$ , while the second clearly cannot be attributed to this.

These observations are in accord with the fact noted in our previous studies<sup>3</sup> that the yield curves for the  $\alpha$ -decay daughter isotopes have a secondary maximum at a bombarding energy about 20 MeV higher than the main peak.

In the case of the radium yield curves we can also point to some interesting features. In most cases it is likely that the radium isotopes are produced by electron-capture decay of the corresponding actinium isotope. When the peaks of the yield curves for radium and actinium isotopes occur at the same bombarding energy, this is presumed to be true, although it is also possible that one proton is evaporated in the de-excitation process leading to formation of radium without the electron capture decay link. This becomes most likely for reactions in which more than three or four neutrons

are evaporated, where the statistical chance of proton emission is increasing, the binding energy of the neutrons is increasing, and the binding energy of protons is decreasing to a very low value. The peak for a (heavy ion,  $pxn$ ) reaction yield would occur rather close to that for a (heavy ion,  $(x+1)n$ ) reaction.

A striking radium yield curve is the one for  $^{214}\text{Ra}$  in the  $^{209}\text{Bi}+^{12}\text{C}$  case as displayed in Fig. 8. As explained in the  $^{214}\text{Ac}$  discussion (Sec. III C), at a  $^{12}\text{C}$  energy below 105 MeV, the  $^{214}\text{Ra}$  yield is linked to  $^{214}\text{Ac}$ , but it clearly departs from it at higher beam energies.

In recent years theoretical discussions of the statistical model treatment of compound-nucleus de-excitation have shown a growing awareness of the role of angular momentum upon the evaporation of protons and  $\alpha$  particles in competition with neutrons and  $\gamma$  rays in the de-excitation of nuclei.<sup>13-17</sup> The anomalies apparent in our francium and radium curves may be a reflection of these angular-momentum effects. Since these results came as a byproduct of the identification work on the new actinium isotopes and were not a main purpose of the research, we do not discuss them further here; but we hope to give them more attention in the future. As a supplement to any future work on this problem, it would be extremely useful to carry out direct measurements on the properties of protons and  $\alpha$  particles emitted in these reactions.

#### ACKNOWLEDGMENTS

The authors wish to thank Albert Ghiorso and Matti Nurmi for encouragement and cooperation throughout this work, especially for suggestions concerning improvements in collection-chamber design. The excellent assistance of the HILAC crew is also gratefully acknowledged.

<sup>13</sup> D. C. Williams and T. D. Thomas, Nucl. Phys. **A92**, 1 (1967).

<sup>14</sup> M. Blann and G. Merkel, Phys. Rev. **137**, B367 (1965).

<sup>15</sup> D. V. Reames, Phys. Rev. **137**, B332 (1965).

<sup>16</sup> S. Jägare, Nucl. Phys. **A95**, 491 (1967).

<sup>17</sup> J. R. Grover and J. Gillat, Phys. Rev. **157**, 802 (1967); **157**, 814 (1967); and **157**, 823 (1967).